

Cyanographone and Isocyanographone – two asymmetrically functionalized graphene pseudohalides and their potential use in chemical sensing

Lukas Eugen Marsoner Steinkasserer* and Beate Paulus

Institut für Chemie und Biochemie, Freie Universität Berlin, Takustraße 3, D-14195 Berlin, Germany

(Dated: March 28, 2017)

I. ABSTRACT

Graphene pseudohalides are natural candidates for use in molecular sensing due to their greater chemical activity as compared to both graphene halides and pristine graphene. Though their study is still in its infancy, being hindered until recently by the unavailability of both selective and efficient procedures for their synthesis, they promise to considerably widen the application potential of chemically modified graphenes. Herein, we employ vdW-DFT to study the structural and electronic properties of two selected graphene pseudohalides namely cyanographone and isocyanographone and investigate the potential use of the latter as a CO sensor in a $N_2/CO_2/O_2$ atmosphere using electron transport calculations.

II. INTRODUCTION

In the wake of the aptly termed *rise of graphene* [1, 2] recent years have seen a growing interest in modifying the properties of graphene, overcoming its weaknesses and subsequently tailoring its properties to specific applications. A promising avenue towards that goal consist in the functionalization of graphene by appropriately chosen chemical groups [3–19]. Among these, atomic substituents such as H, F, Cl and Br have attracted large amounts of attention, especially in the theoretical community, as they allow for a relatively simple and controlled modification of graphene properties and lend themselves well to computational study [20, 21].

Though the interest in graphene halides has been extensive, little attention has as of yet been paid to its pseudohalide derivatives [13]. This is in part due to the fact that, until very recently, no synthetic protocols were in place which allowed for the efficient and selective synthesis of such derivatives [15]. Pseudohalogens, e.g. N_3 , SCN, CN, while presenting many of the attractive chemical properties of halogen atoms, making them suitable for use in graphene functionalization, at the same time offer much greater chemical activity than true halogens. While there is in principle a wide variety of pseudohalides available, herein we will focus solely on the cyano group (CN) and two possible derivatives that can be formed from it, i.e., cyanographone (GrCN) and isocyanographone (GrNC) in which the cyano group binds

to the graphene layer via the carbon and nitrogen atom respectively.

Cyanographone has very recently been synthesized for the first time by Bakandritsos and coworkers via the reaction of NaCN with fluorographene [15]. While experimental results indicate a functionalization degree of 15%, herein we will only consider stoichiometric derivatives. Moreover, while symmetrically functionalized materials are certainly interesting they, just as most graphene halides, have the disadvantage of being rather wide band gap semiconductors – making them unappealing for many potential applications. One way to overcome this problem consists in asymmetrical functionalization on just one side of the graphene layer. We will, in analogy to half-hydrogenated graphene, use the suffix *-one* to indicate such half-functionalized graphene pseudohalides. Half-cyanated graphene will therefore be termed *cyanographone* while half-isocyanated graphene is referred to as *isocyanographone*. Apart from analyzing the structural and electronic properties of the pristine and BN adsorbed cyano- and isocyanographone layers we will, for the case of cyanographone, see how adsorption of gas molecules can significantly alter its electronic properties rendering it an interesting target for the development of nanoscale chemical sensors.

Gas sensors play a crucial role in a variety of fields, ranging from scientific research to industrial or domestic activities [22–24]. In recent years a growing number of researchers have become interested in exploiting the attractive properties of 2D materials such as their extremely high surface to volume ratios, for the detection of rarefied gases with the promise of achieving measurement accuracy down to individual molecules [25–28]. One of the main challenges facing the application of 2D materials to gas sensing though, consist in selectively detecting only specific types of molecules. While e.g. great progress has been made in the field of graphene-based sensors [29–35], most common gas species are only weakly adsorbed on the graphene surface [36, 37], thereby increasing the risk of cross-sensitivity. Herein, focusing on the problem of carbon monoxide detection, we will show how BN adsorbed cyanographone (GrCN@BN) is able to strongly bind to CO, while at the same time only weakly interacting with a number of other molecules i.e. N_2 , O_2 and CO_2 . This disparate interaction behavior in turn leads to qualitatively different changes to the systems $I - V$ curve, making it possible to selectively detect CO even in the presence of other common atmospheric gases.

* marsoner@zedat.fu-berlin.de

III. COMPUTATIONAL DETAILS

All calculations in this work were performed using the GPAW program [38–41]. If not otherwise stated, all calculations employed the libvdwxc [42] implementation of the vdW-DF-CX functional by Berland and Hyldgaard [43–46] which allows for a consistent description of non-local vdW-forces within the framework of density functional theory. We note at this point that in the case of spin-polarized calculations, the total density was used to evaluate the non-local vdW correlation.

During structure optimization, atomic positions were relaxed until the remaining forces were below 0.05 eV/Å, while unit cell parameters were obtained from parabolic fits of energies around the minimum. Unless otherwise stated, all calculations were performed using a real-space grid representation of the wave functions with a grid spacing of 0.15 Å (rounded slightly in order to match the unit cell) and employed at least a 24×24 Γ -centered Monkhorst-Pack grid.

Structure optimizations on supercells used to study molecular adsorption were done using GPAW's LCAO mode [47] employing a double- ζ polarized (dzp) basis set. Unit cell parameters were kept constant during the relaxation while atomic positions were allowed to relax until remaining forces were below 0.05 eV/Å. Binding energies were again obtained from the more accurate real-space grid method. While structure optimizations employed a Γ -centered 4×4 Monkhorst-Pack grid for the 3×3 supercell, in the case of binding energies a Γ -centered 8×8 grid was used.

Finally, electronic transport calculations were done via the ASE [48, 49] implementation of the Green's function formalism (see ref. [50–53] for details on the method and implementation). The Hamiltonians and overlap matrices are obtained from LCAO calculations employing the the vdW-DF-CX functional with a dzp basis set. The computational cell was sampled using 4 Monkhorst-Pack k -grid points along the periodic direction.

IV. RESULTS AND DISCUSSION

A. Symmetric and asymmetric functionalization

As shown in fig. 1, we initially considered both symmetrically (Gr2CN, Gr2NC) and asymmetrically saturated (GrCN, GrNC) graphene derivatives. The former can be expected to display an electronic structure analogous to that of *ordinary* graphene halides such as fluorographene [7, 54, 55] and graphane [56–58], characterized by rather large band gaps. To verify this, we calculated the quasiparticle gaps of the aforementioned systems using the GLLB-SC functional by Kuisma et al. [59, 60] which has been shown to yield excellent agreement with experimental results for a large number of systems [61].

As expected, we find Gr2CN/Gr2NC both to be wide band gap semiconductors with Gr2CN having a

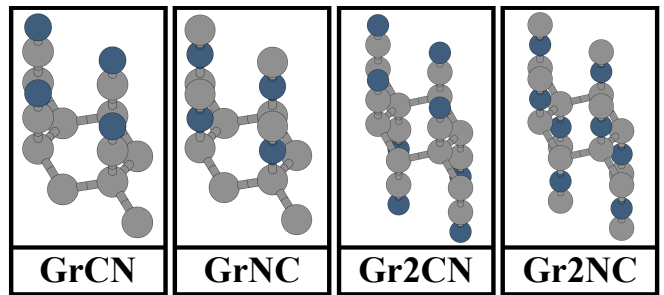


FIG. 1. Summary of the different types of functionalization considered, together with the associated designations which will be used throughout this work. GrCN and GrNC refer to cyanographone and isocyanographone while labels Gr2CN and Gr2NC are used to indicate cyanographene and isocyanographene respectively. In all cases, carbon atoms are drawn in gray while nitrogen atoms are shown in dark blue.

GLLB-SC+ Δ_{xc} quasiparticle gap equal to 3.9 eV while Gr2NC shows a gap of 3.4 eV. Given that their large band gap makes them unappealing for a number of important potential applications such as photovoltaics or chemical sensing, we will not consider the fully saturated cases any further, focusing rather on the more interesting half-functionalized systems. These asymmetrically saturated structures contain an unpaired electron on one of the two graphene sublattices (the other being functionalized by the cyano group), which makes them analogous to half-hydrogenated/-fluorinated graphene, i.e., graphone/fluorographene [62–72].

GrCN	Spin state	GrNC
-759 meV (-908 meV)		-1248 meV (-1420 meV)
-801 meV (-939 meV)		-1326 meV (-1488 meV)

FIG. 2. Stability of different spin-phases of GrCN and GrNC. The central image shows a schematic representation of the ferromagnetic (bottom line) as well as antiferromagnetic (upper line) spin orientation. Energies are given relative to the spin-paired case. Pairs of values correspond to results obtained using the vdW-DF-CX and PBE functional respectively with the latter being shown in parenthesis. Note that for vdW-DF-CX, the total density was used to evaluate the non-local vdW correlation.

Given this structure one would naturally expect them to display some form of long-range magnetic ordering. To confirm this, we performed vdW-DF-CX and PBE [73] calculations on a 2×2 supercell of GrCN and GrNC considering both ferromagnetic as well as antiferromag-

netic ordering of the unpaired electrons and comparing their energy to that of the spin-paired state. The results of these calculations are shown in fig. 2 which shows that, in accordance with graphone, both cyanographone (GrCN) and isocyanographone (GrNC) display a ferromagnetic ground state. This stands in contrast to the case of half-fluorinated graphene [68, 72] where ferromagnetic ordering of the spins does not correspond to the lowest energy state of the system. Of the two systems considered (GrCN and GrNC), GrCN is more stable than GrNC by ≈ 0.7 eV/unit cell with vdW-DF-CX and PBE results differing only slightly.

V. STABILITY

One of the main challenges of partially-saturated graphene derivatives is their relatively low stability compared to fully-functionalized systems. For the case of graphone, Hemmatiyani et al. proposed that stability might be significantly enhanced by depositing the material on hexagonal boron nitride (BN) [70].

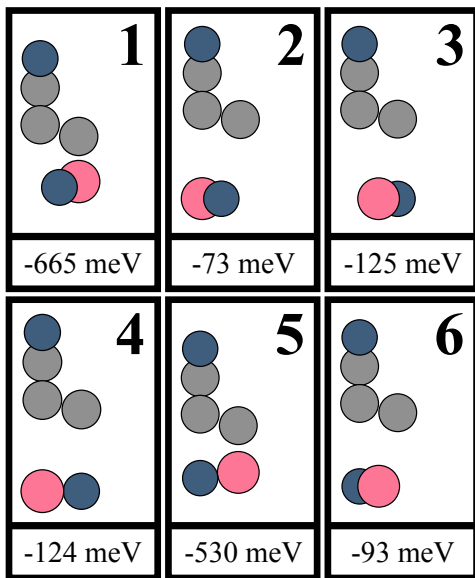


FIG. 3. Relaxed structures for unit cells with different high-symmetry orientations of the GrCN@BN bilayer. Nitrogen atoms are shown in blue, while boron atoms are shown in rose and carbon atoms in gray. Note that in the case of adsorption position 1 the buckling of the graphene layer is ≈ 0.5 Å as compared to ≈ 0.4 Å in the freestanding case. Adsorption on top of a nitrogen atom has almost no influence on the buckling and e.g. structure 3 shows the same level of buckling as the freestanding GrCN layer. The binding energy for each structure is given per unit cell.

We mention at this point that the lattice mismatch between GrCN/GrNC and BN is $\approx 5\%$. While the difference is rather small, it would at the same time result in long-range Moiré superlattices which might show locally different electronic properties, making practical applica-

tions of the materials more difficult. Fortunately, both cyanographone and isocyanographone bind strongly to the BN substrate (see fig. 3), making the emergence of large-scale Moiré structures less likely. In our calculations we have in all cases fixed the lattice constant of the GrCN/GrNC@BN bilayer to that of GrCN/GrNC respectively.

As a first step in considering the influence of BN adsorption on the stability of GrCN/GrNC we performed a series of calculations for different relative orientations of the two monolayers. This analysis was only done for GrCN as conclusions are expected to be applicable also to GrNC. The results (which are summarized in fig. 3) show a clear preference for the carbon atom containing the unpaired electron to be adsorbed on top of the boron atom. This can be explained by the formation of a covalent bond between the electron-rich carbon atom and the relatively electron-poor boron atom within the BN layer. For the boron adsorption site, the position of the nitrogen atom on the other hand has a much smaller influence on the binding energy (compare orientations 1 and 5 in fig. 3). Still the system shows a clear minimum (orientation 1 in fig. 3) which is ≈ 130 meV per unit cell more stable than the second most stable structure (orientation 5 in fig. 3).

It is worth noting that the formation of the carbon-boron bond leads to a suppression of the GrCN magnetic moment while at the same time, the system maintains its conducting nature, as is shown in fig. 4.

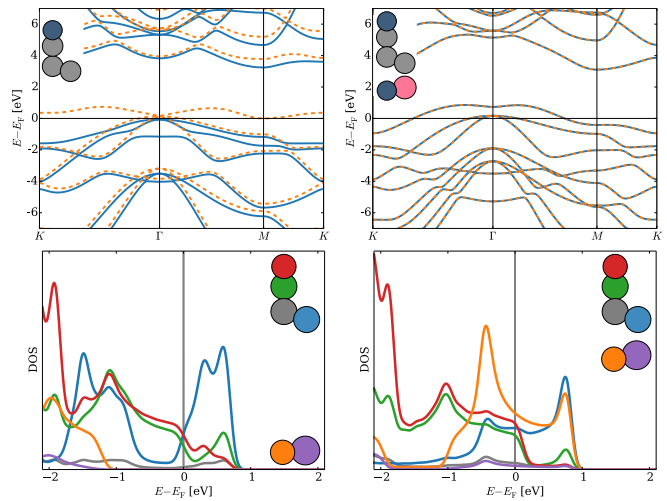


FIG. 4. The two top figures show vdW-DF-CX band structures for freestanding and BN deposited cyanographone demonstrating the loss of magnetization upon adsorption while at the same time, metallicity is conserved. Insets show the respective atomic structures and solid-blue/dashed-orange lines correspond to the majority/minority spin channels respectively. The two bottom figures show the DOS for the same structures with curves corresponding to projections onto individual atoms. For ease of comparison between the two DOS, we have added a BN layer at a distance of 20 Å from the isolated GrCN layer.

Figure 4 also shows the local DOS for the two systems which provides us with some additional information as to the nature of the changes to the GrCN electronic structure upon BN adsorption. Focusing first on freestanding GrCN, we see that, though the unpaired electron on the carbon atom labeled in blue contributes most strongly to the conduction bands close to E_F , the CN group (green and red curves) provides the largest contribution to the region immediately below the Fermi energy. The BN layer on the other hand, which we have added to the structure at a distance of 20 Å to avoid any residual interaction between the two layers, shows no significant DOS around the Fermi level.

As the two layers are put into contact, the situation changes drastically. A chemical bond is formed between GrCN and BN and the formerly unpaired electrons' contribution to the DOS around E_F decreases. At the same time the BN layer, which before did not contribute to the DOS in the vicinity of E_F , now shows a strong contribution on the part of the nitrogen atom (orange curve). The boron atom (violet curve) on the other hand remains close to insignificant in the valence region, contributing only very little to the overall DOS.

To investigate the binding energy of CN to graphene in the case of GrCN and GrNC and to ascertain whether, as in the case of graphone, BN adsorption might be used to increase the stability of the two systems, we performed a series of energy scans for the CN – graphene distance. The resulting potential energy surfaces (PES) are shown in fig. 5. We see that, as in the case of graphone, both cyanographone and isocyanographone can be strongly stabilized by adsorption on BN. While the former shows a binding energy > 1 eV, the latter, though stabilized, still shows very low thermodynamic stability. This being said, the energy barrier for the dissociation of BN adsorbed isocyanographone into its constituent species is close to 1 eV, meaning the system could potentially show significant kinetic stability.

In the following we will nonetheless limit ourselves to considering only GrCN@BN when studying the adsorption of gas molecules since its higher thermodynamic stability makes it more likely to be stable under realistic conditions.

VI. INTERACTIONS WITH GAS MOLECULES

In order to demonstrate the ability of GrCN@BN sensors to discriminate between different molecules based on whether or not they interact strongly with the materials cyano groups, we will consider the problem of the selective detection of CO in the presence of CO₂, N₂ as well as O₂. To study the effects of this interaction, we analyze the molecules' interaction with a model GrCN@BN detector and calculate its current–voltage characteristics ($I - V$ curves) before and after gas adsorption.

In order to study molecular adsorption, we constructed a 3×3 supercell of GrCN@BN. For each of the four

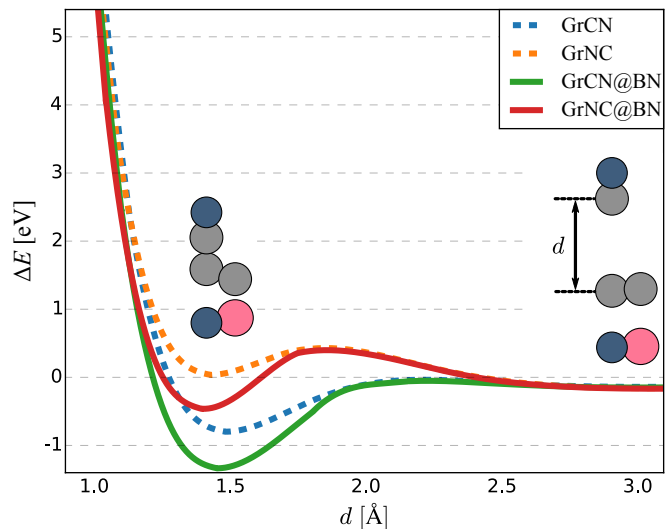


FIG. 5. Potential energy surface scan for CN/NC adsorption on both freestanding (GrCN/GrNC) as well as BN adsorbed graphene (GrCN@BN/GrNC@BN). The relative orientation of graphene and BN corresponds to the most stable GrCN@BN system (orientation 1 in fig. 3). All calculations are performed using the vdW-DF-CX functional and energies are given relative to the values at $d \approx 6$ Å.

molecules studied we then considered two different initial positions, i.e., on top of a CN group as well as in the center of a six-membered carbon ring (see fig. 6). For each of these two initial positions we further considered two different orientations of the molecule. We then allowed the structures to relax while keeping the unit cell parameters fixed.

	CO	CO ₂	O ₂	N ₂
P1 _R	-1951	-93	-423	-31
P2 _R	-83	-216	-464	-105
P1 _{CN}	-1283	-121	-381	-65
P2 _{CN}	-151	-207	-481	-108

TABLE I. vdW-DF-CX binding energies for CO, CO₂, O₂ and N₂ on GrCN@BN. All calculations are performed using a 3×3 supercell and values are given in meV. Position labels **R** and **CN** refer to starting positions of the structure optimization with the molecule either in the center of a six-membered carbon-ring or on top of a CN group, while P1/P2 have slightly different meanings in the cases of CO and CO₂/N₂/O₂ respectively. For CO, P1/P2 indicate whether the carbon/oxygen atom respectively is pointing towards GrCN@BN while for CO₂/N₂/O₂, P1 corresponds to the molecular axis being *orthogonal* to the plane of the GrCN@BN layer while P2 refers to the axis being *parallel* to it.

The final binding energies for all relaxed structures are shown in table I. We see that, while CO₂ and N₂ are only weakly adsorbed on GrCN@BN, both O₂ and CO interact more strongly with the (P1) CO adsorption en-

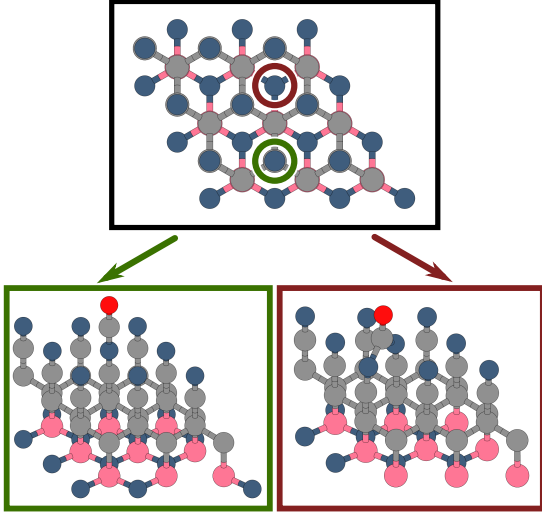


FIG. 6. The black frame shows a top view of the 3×3 GrCN@BN supercell used in the calculations where the two starting positions for the adsorbed molecules (**R** and **CN** in table I) have been indicated by red and green circles respectively. The bottom frames show the corresponding relaxed geometries for the case of CO adsorption in the P1 orientation. Note how in the case of the **R** starting position, the CO molecule has moved away from the center of the six-membered carbon ring into a bridging position between two nitrogen atoms on neighboring CN groups.

ergies being $\approx 3 - 4\times$ larger than those of O_2 . For O_2 , both the relatively high interaction energy, as well as its only weak dependence on the orientation of the molecule likely indicate the presence of some electrostatic interaction between the molecule and the surface cyano groups. As we will see later though, this stronger interaction as compared to CO_2 and N_2 , has only a small influence on the transport properties of O_2 doped GrCN@BN. In the case of CO on the other hand, a chemical bond is formed between the CO carbon atom and one (P1_{CN}) or two (P1_R) surface CN groups, the latter configuration being more stable than the former by ≈ 650 meV. CO-orientations for which the oxygen atom is pointed towards the GrCN@BN surface (P2) show only weak binding similar to that of N_2 and CO_2 .

VII. CURRENT-VOLTAGE CHARACTERISTICS

Let us now conclude our study by analyzing the simplified model of a GrCN@BN based gas sensor shown in fig. 7. To study the ability of GrCN@BN to selectively detect CO in the presence of CO_2 , O_2 and N_2 , we calculate the current-voltage characteristics ($I - V$ curves) of both pristine as well as molecularly doped GrCN@BN. After computing the transmission using the Green's function formalism as implemented in ASE, the current (I) can be obtained as a function of the applied voltage (V)

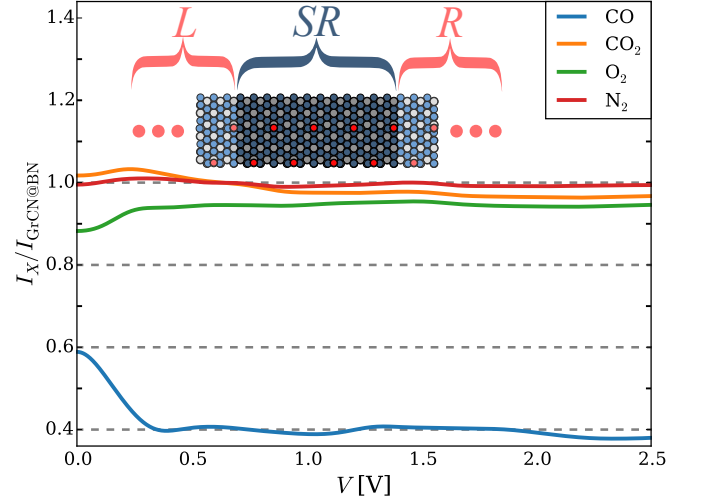


FIG. 7. Voltage-dependent currents, $I_X/I_{\text{GrCN@BN}}$ at $T = 300$ K, where $X = \text{CO}, \text{CO}_2, \text{O}_2, \text{N}_2$ as obtained from the Landauer equation (eq. 1). In all cases, results refer to the most stable adsorption position of the molecule on the surface (see table I). The inset depicts a schematic representation of the computational setup used in the transport calculations where the central scattering region (**SR**), consists of four orthorhombic cells corresponding to the 3×3 supercell of (molecularly doped) GrCN@BN, depicted in fig. 6. The desaturated regions to the left and right of the scattering region correspond to the two semi-infinite leads (**L/R**) and consist of a single orthorhombic cell of the same type as those constituting the scattering region.

from the standard Landauer equation as

$$I(V) = \frac{2e}{h} \int_{-\infty}^{\infty} dE [f_{\text{L}}(E, \mu_{\text{L}}(V)) - f_{\text{R}}(E, \mu_{\text{R}}(V))] T(E) \quad (1)$$

where $f_{\text{L/R}}$ are the Fermi-Dirac distributions for the left and right lead respectively and the lead chemical potentials are chosen to be $\mu_{\text{L/R}} = E_{\text{F}} \pm V/2$ with E_{F} being the Fermi energy. While the voltage is applied from left to right, the entire structure is periodic in the orthogonal direction which is sampled by **k**-points [53].

To determine whether GrCN@BN devices might be useful as chemical sensors, we are not primarily interested in the *absolute* value of the current in the molecularly doped layers, but rather its *relative* magnitude as compared to the pristine system ($I_{\text{GrCN@BN}}$). When analyzing the corresponding curves, shown in fig. 7, it becomes clear that adsorption of both CO_2 and N_2 leaves the systems transport properties largely unaltered. O_2 adsorption does lead to some changes in the current at low voltages, but for $V \geq 0.25$ V, the reduction in current again becomes small and close to that seen for N_2 and CO_2 . In contrast, CO adsorption causes a much more significant reduction in the current, lowering it to $\approx 40\%$ of its GrCN@BN value. This decrease in current upon CO adsorption is also largely constant, meaning that a possible detector could be operated within a range of

voltages.

The clear distinction between the $I-V$ curves of CO_2 , O_2 and N_2 adsorbed systems on the one hand, and CO adsorbed ones on the other, demonstrates the potential of GrCN@BN to be used as a chemical sensor for CO detection within a $\text{CO}_2/\text{O}_2/\text{N}_2$ atmosphere. A detailed study of other molecular species is of course needed both to identify additional potential uses as well as reveal possible issues arising from cross-sensitivity to other strongly adsorbed species.

VIII. CONCLUSIONS

We have demonstrated how half-cyanation of graphene leads to a thermodynamically stable material which is conducting and shows long-range ferromagnetic ordering. This material was termed *cyanographone* in analogy to half-hydrogenated graphene (graphene). We subsequently showed how the material can be further stabilized by depositing it on hexagonal BN. The deposition leads to the formation of a chemical bond between the unsaturated carbon sub-lattice of the cyanographone, and the boron atoms within the BN layer. This in turn not only stabilizes the cyanographone monolayer but further causes suppression of the ferromagnetic ordering observed for the freestanding system, without though leading to the opening of a band gap. Lastly, we investigated the chemical sensing capabilities of this new-found material by studying the changes in its current-voltage characteristic upon adsorption of different common gas molecules. We found that, while CO_2 , O_2 and N_2 interact weakly with GrCN@BN and only cause rather small changes to its $I-V$ curve, in the case of CO adsorp-

tion, a chemical bond is formed between the molecule and the surface, resulting in a reduction of the current to $\approx 40\%$ of its value for the pristine system, over a range of voltages. The strength of this response as well as its approximate voltage-independence make the use of BN deposited cyanographone as a chemical sensor for CO detection within a $\text{CO}_2/\text{O}_2/\text{N}_2$ atmosphere an attractive proposition.

As the application of GrCN@BN to CO detection likely by no means exhausts the entirety of its possible uses, we hope that our study, in combination with the recent advancements in cyanographene synthesis, will spur more research into pseudohalogenated graphenes in general as well as cyanographone in particular, helping to fully uncover the potential of this fascinating class of materials.

ACKNOWLEDGMENTS

LEMS acknowledges financial support by the Studienstiftung des deutschen Volkes e.V., the international Max Planck Research School "Complex Surfaces in Material Sciences" as well as the Deutsche Forschungsgemeinschaft within the Priority Program (SPP) 1459 (Graphene). The North-German Supercomputing Alliance (HLRN) and computer facilities of the Freie Universität Berlin (ZEDAT) are acknowledged for computer time. The authors thank Vincent Pohl (Berlin) for help with the electronic transport calculations, Ask Hjorth Larsen (Donostia-San Sebastián) for helpful discussions regarding vdW-DF-CX as well as Carmen Reden (Berlin) for proofreading this manuscript.

The XCrySDen package [74, 75] and ASE [48, 49] were used to create images of atomic structures throughout this work while plots were created using Matplotlib [76].

-
- [1] A. K. Geim and K. S. Novoselov, *Nature Materials* **6**, 183 (2007).
 - [2] K. S. Novoselov, A. K. Geim, S. V. Morozov, D. Jiang, Y. Zhang, S. V. Dubonos, I. V. Grigorieva, and A. A. Firsov, *Science* **306**, 666 (2004).
 - [3] C. K. Chua and M. Pumera, *Chem. Soc. Rev.* **42**, 3222 (2013).
 - [4] F. Karlický, E. Otyepková, R. Lo, M. Pitoňák, P. Jurečka, M. Pykal, P. Hobza, and M. Otyepka, *J. Chem. Theory Comput.* **13**, 1328 (2017).
 - [5] L. Liao, H. Peng, and Z. Liu, *J. Am. Chem. Soc.* **136**, 12194 (2014).
 - [6] S. Eigler and A. Hirsch, *Angew. Chem. Int. Ed.* **53**, 7720 (2014).
 - [7] J. T. Robinson, J. S. Burgess, C. E. Junkermeier, S. C. Badescu, T. L. Reinecke, F. K. Perkins, M. K. Zalalutdinov, J. W. Baldwin, J. C. Culbertson, P. E. Sheehan, and E. S. Snow, *Nano Lett.* **10**, 3001 (2010).
 - [8] A. Criado, M. Melchionna, S. Marchesan, and M. Prato, *Angew. Chem. Int. Ed.* **54**, 10734 (2015).
 - [9] T. Kuila, S. Bose, A. K. Mishra, P. Khanra, N. H. Kim, and J. H. Lee, *Prog. Mater. Sci.* **57**, 1061 (2012).
 - [10] V. Georgakilas, M. Otyepka, A. B. Bourlinos, V. Chandra, N. Kim, K. C. Kemp, P. Hobza, R. Zbořil, and K. S. Kim, *Chem. Rev.* **112**, 6156 (2012).
 - [11] A. L. Ivanovskii, *Russ. Chem. Rev.* **81**, 571 (2012).
 - [12] J. E. Johns and M. C. Hersam, *Acc. Chem. Res.* **46**, 77 (2013).
 - [13] F. Karlický, K. K. R. Datta, M. Otyepka, and R. Zbořil, *ACS Nano* **7**, 6434 (2013).
 - [14] J. Tuček, K. Holá, A. B. Bourlinos, P. Błoński, A. Bakandritsos, J. Ugolotti, M. Dubecký, F. Karlický, V. Ranc, K. Čépe, M. Otyepka, and R. Zbořil, *Nat. Commun.* **8**, 14525 (2017).
 - [15] A. Bakandritsos, M. Pykal, P. Błoński, P. Jakubec, D. D. Chronopoulos, K. Poláková, V. Georgakilas, K. Čépe, O. Tomanec, V. Ranc, A. B. Bourlinos, R. Zbořil, and M. Otyepka, *ACS Nano*, null (2017).
 - [16] A. B. Bourlinos, K. Safarova, K. Siskova, and R. Zbořil, *Carbon* **50**, 1425 (2012).
 - [17] A. Setaro, M. Adeli, M. Glaeske, D. Przyrembel, T. Bisswanger, G. Gordeev, F. Maschietto, A. Faghani,

- B. Paulus, M. Weinelt, R. Arenal, R. Haag, and S. Reich, *Nat. Commun.* **8**, 14281 (2017).
- [18] G. L. C. Paulus, Q. H. Wang, and M. S. Strano, *Acc. Chem. Res.* **46**, 160 (2013).
- [19] J. Liu, J. Tang, and J. J. Gooding, *J. Mater. Chem.* **22**, 12435 (2012).
- [20] T. Zhang, Q. Xue, S. Zhang, and M. Dong, *Nano Today* **7**, 180 (2012).
- [21] M. Pykal, P. Jurečka, F. Karlický, and M. Otyepka, *Phys. Chem. Chem. Phys.* **18**, 6351 (2016).
- [22] S. Capone, A. Forleo, L. Francioso, R. Rella, P. Siciliano, J. Spadavecchia, D. S. Presicce, and A. M. Taurino, *ChemInform* **35**, 1335 (2004).
- [23] G. Sberveglieri, ed., *Gas Sensors* (Springer Nature, 1992).
- [24] P. T. Moseley, *Meas. Sci. Technol.* **8**, 223 (1997).
- [25] S. Varghese, S. Varghese, S. Swaminathan, K. Singh, and V. Mittal, *Electron.* **4**, 651 (2015).
- [26] L. Kou, T. Frauenheim, and C. Chen, *J. Phys. Chem. Lett.* **5**, 2675 (2014).
- [27] A. N. Abbas, B. Liu, L. Chen, Y. Ma, S. Cong, N. Aroonyadet, M. Köpf, T. Nilges, and C. Zhou, *ACS Nano* **9**, 5618 (2015).
- [28] K. Lee, R. Gatenby, N. McEvoy, T. Hallam, and G. S. Duesberg, *Adv. Mater.* **25**, 6699 (2013).
- [29] F. Schedin, A. K. Geim, S. V. Morozov, E. W. Hill, P. Blake, M. I. Katsnelson, and K. S. Novoselov, *Nat. Mater.* **6**, 652 (2007).
- [30] T. Wang, D. Huang, Z. Yang, S. Xu, G. He, X. Li, N. Hu, G. Yin, D. He, and L. Zhang, *Nano-Micro Lett.* **8**, 95 (2015).
- [31] W. Yuan and G. Shi, *J. Mater. Chem. A* **1**, 10078 (2013).
- [32] B. Huang, Z. Li, Z. Liu, G. Zhou, S. Hao, J. Wu, B.-L. Gu, and W. Duan, *J. Phys. Chem. C* **112**, 13442 (2008).
- [33] J. T. Robinson, F. K. Perkins, E. S. Snow, Z. Wei, and P. E. Sheehan, *Nano Lett.* **8**, 3137 (2008).
- [34] R. Bogue, *Sens. Rev.* **34**, 1 (2014).
- [35] Q. He, S. Wu, Z. Yin, and H. Zhang, *Chem. Sci.* **3**, 1764 (2012).
- [36] O. Leenaerts, B. Partoens, and F. M. Peeters, *Phys. Rev. B* **77**, 125416 (2008).
- [37] T. O. Wehling, K. S. Novoselov, S. V. Morozov, E. E. Vdovin, M. I. Katsnelson, A. K. Geim, and A. I. Lichtenstein, *Nano Lett.* **8**, 173 (2008).
- [38] J. J. Mortensen, L. B. Hansen, and K. W. Jacobsen, *Phys. Rev. B* **71**, 035109 (2005).
- [39] J. Enkovaara, C. Rostgaard, J. J. Mortensen, J. Chen, M. Dulak, L. Ferrighi, J. Gavnholt, C. Glinsvad, V. Haikola, H. A. Hansen, H. H. Kristoffersen, M. Kuisma, A. H. Larsen, L. Lehtovaara, M. Ljungberg, O. Lopez-Acevedo, P. G. Moses, J. Ojanen, T. Olsen, V. Petzold, N. A. Romero, J. Stausholm-Møller, M. Strange, G. A. Tritsarlis, M. Vanin, M. Walter, B. Hammer, H. Häkkinen, G. K. H. Madsen, R. M. Nieminen, J. K. Nørskov, M. Puska, T. T. Rantala, J. Schiøtz, K. S. Thygesen, and K. W. Jacobsen, *J. Phys. Condens. Matter* **22**, 253202 (2010).
- [40] M. A. Marques, M. J. Oliveira, and T. Burnus, *Comput. Phys. Commun.* **183**, 2272 (2012).
- [41] P. E. Blöchl, *Phys. Rev. B* **50**, 17953 (1994).
- [42] A. H. Larsen, M. Kuisma, J. Löfgren, Y. Pouillon, P. Erhart, and P. Hyldgaard, *arXiv preprint arXiv:1703.06999* (2017).
- [43] K. Berland, C. A. Arter, V. R. Cooper, K. Lee, B. I. Lundqvist, E. Schröder, T. Thonhauser, and P. Hyldgaard, *J. Chem. Phys.* **140**, 18A539 (2014).
- [44] K. Berland and P. Hyldgaard, *Phys. Rev. B* **89**, 035412 (2014).
- [45] G. Román-Pérez and J. M. Soler, *Phys. Rev. Lett.* **103**, 096102 (2009).
- [46] L. Gharaee, P. Erhart, and P. Hyldgaard, *Phys. Rev. B* **95**, 085147 (2017).
- [47] A. H. Larsen, M. Vanin, J. J. Mortensen, K. S. Thygesen, and K. W. Jacobsen, *Phys. Rev. B* **80**, 195112 (2009).
- [48] S. Bahn and K. Jacobsen, *Comput. Sci. Eng.* **4**, 56 (2002).
- [49] A. H. Larsen, J. J. Mortensen, J. Blomqvist, I. E. Castelli, R. Christensen, M. Dulak, J. Friis, M. N. Groves, B. Hammer, C. Hargus, E. D. Hermes, P. C. Jennings, P. B. Jensen, J. Kermode, J. R. Kitchin, E. L. Kolsbjerg, J. Kubala, S. Lysgaard, J. B. Maronsson, T. Maxson, T. Olsen, L. Pastewka, A. Peterson, C. Rostgaard, J. Schiøtz, O. Schütt, M. Strange, K. Thygesen, T. Vegge, L. Vilhelmsen, M. Walter, Z. Zeng, and K. W. Jacobsen, *Ψ_k Scientific Highlight Of The Month* (2017).
- [50] M. Strange, I. S. Kristensen, K. S. Thygesen, and K. W. Jacobsen, *J. Chem. Phys.* **128**, 114714 (2008).
- [51] K. S. Thygesen, M. V. Bollinger, and K. W. Jacobsen, *Phys. Rev. B* **67**, 115404 (2003).
- [52] K. S. Thygesen and K. W. Jacobsen, *Chem. Phys.* **319**, 111 (2005).
- [53] K. S. Thygesen and K. W. Jacobsen, *Phys. Rev. B* **72**, 033401 (2005).
- [54] R. Zboril, F. Karlický, A. B. Bourlinos, T. A. Steriotis, A. K. Stubos, V. Georgakilas, K. Šafářová, D. Jančík, C. Trapalis, and M. Otyepka, *Small* **6**, 2885 (2010).
- [55] R. R. Nair, W. Ren, R. Jalil, I. Riaz, V. G. Kravets, L. Britnell, P. Blake, F. Schedin, A. S. Mayorov, S. Yuan, M. I. Katsnelson, H.-M. Cheng, W. Strupinski, L. G. Bulusheva, A. V. Okotrub, I. V. Grigorieva, A. N. Grigorenko, K. S. Novoselov, and A. K. Geim, *Small* **6**, 2877 (2010).
- [56] D. C. Elias, R. R. Nair, T. M. G. Mohiuddin, S. V. Morozov, P. Blake, M. P. Halsall, A. C. Ferrari, D. W. Boukhvalov, M. I. Katsnelson, A. K. Geim, and K. S. Novoselov, *Science* **323**, 610 (2009).
- [57] J. O. Sofo, A. S. Chaudhari, and G. D. Barber, *Phys. Rev. B* **75**, 153401 (2007).
- [58] M. H. F. Sluiter and Y. Kawazoe, *Phys. Rev. B* **68**, 085410 (2003).
- [59] M. Kuisma, J. Ojanen, J. Enkovaara, and T. T. Rantala, *Phys. Rev. B* **82**, 115106 (2010).
- [60] O. Gritsenko, R. van Leeuwen, E. van Lenthe, and E. J. Baerends, *Phys. Rev. A* **51**, 1944 (1995).
- [61] I. E. Castelli, T. Olsen, S. Datta, D. D. Landis, S. Dahl, K. S. Thygesen, and K. W. Jacobsen, *Energy Environ. Sci.* **5**, 5814 (2012).
- [62] E. Şaşıoğlu, H. Hadipour, C. Friedrich, S. Blügel, and I. Mertig, *Phys. Rev. B* **95**, 060408 (2017).
- [63] F. Buonocore, A. M. Conte, and N. Lisi, *Physica E* **78**, 65 (2016).
- [64] J. Zhou, Q. Wang, Q. Sun, and P. Jena, *Appl. Phys. Lett.* **98**, 063108 (2011).
- [65] A. I. Podlivaev and L. A. Openov, *Semiconductors* **45**, 958 (2011).
- [66] C. F. Woellner, P. A. da Silva Autreto, and D. S. Galvao, *arXiv preprint arXiv:1606.09235* (2016).
- [67] C. F. Woellner, P. A. da Silva Autreto, and D. S. Galvao, *arXiv preprint arXiv:1601.04484* (2016).

- [68] Q. Peng, J. Crean, L. Han, S. Liu, X. Wen, S. De, and A. Dearden, [Nanotechnol. Sci. Appl.](#), **1** (2014).
- [69] H. Şahin, M. Topsakal, and S. Ciraci, [Phys. Rev. B](#) **83**, 115432 (2011).
- [70] S. Hemmatiyani, M. Polini, A. Abanov, A. H. MacDonald, and J. Sinova, [Phys. Rev. B](#) **90**, 035433 (2014).
- [71] S. C. Ray, N. Soin, T. Makgato, C. H. Chuang, W. F. Pong, S. S. Roy, S. K. Ghosh, A. M. Strydom, and J. A. McLaughlin, [Sci. Rep.](#) **4**, 3862 (2014).
- [72] D. Boukhvalov, [Physica E](#) **43**, 199 (2010).
- [73] J. P. Perdew, K. Burke, and M. Ernzerhof, [Phys. Rev. Lett.](#) **77**, 3865 (1996).
- [74] A. Kokalj, [Computational Materials Science](#) **28**, 155 (2003).
- [75] A. Kokalj, [Journal of Molecular Graphics and Modelling](#) **17**, 176 (1999).
- [76] J. D. Hunter, [Comput. Sci. Eng.](#) **9**, 90 (2007).